A multicell structural battery composite laminate

Received: 19 October 2021 | Revised: 16 November 2021 | Accepted: 19 December 2021

DOI: 10.1002/eom2.12180

RESEARCH ARTICLE

EcoMat FUNCTIONAL MATERIALS FOR GREEN ENERGY AND ENVIRONMENT WILEY

A multicell structural battery composite laminate

Johanna Xu[1] | **Zeyang Geng**[2] | **Marcus Johansen**[1] | **David Carlstedt**[1] | **Shanghong Duan**[1] | **Torbjörn Thiringer**[2] | **Fang Liu**[1] | **Leif E. Asp**[1]

[1]Department of Industrial and Materials Science, Chalmers University of Technology, Gothenburg, Sweden

[2]Department of Electrical Engineering, Chalmers University of Technology, Gothenburg, Sweden

Correspondence
Johanna Xu and Leif E. Asp, Department of Industrial and Materials Science, Chalmers University of Technology, Gothenburg SE-412 96, Sweden.
Email: johannax@chalmers.se and leif.asp@chalmers.se

Funding information
VINNOVA; Swedish National Space Agency, Grant/Award Number: 2020-00256; National Swedish Energy Administration, Grant/Award Number: 42789-1; USAF, Grant/Award Number: FA8655-21-1-7038; European Union, Clean Sky Joint Undertaking 2, Horizon 2020, Grant/Award Number: 738085

Abstract

Multifunctional materials facilitate lightweight and slender structural solutions for numerous applications. In transportation, construction materials that can act as a battery, and store electrical energy, will contribute to realization of highly energy efficient vehicles and aircraft. Herein, a multicell structural battery composite laminate, with three state-of-the-art structural battery composite cells connected in series is demonstrated. The experimental results show that the capacity of the structural battery composite cells is only moderately affected by tensile loading up to 0.36% strain. The multicell structural battery laminate is made embedding the three connected structural battery composite cells between carbon fiber/glass fiber composite face sheets. Electrochemical performance of the multicell structural battery is demonstrated experimentally. High charge transfer resistance for the pack as well as the individual cells is reported. Mechanical performance of the structural battery laminate is estimated by classical laminate theory. Computed engineering in-plane moduli for the multicell structural battery laminate are on par with conventional glass fiber composite multiaxial laminates.

KEYWORDS

biomimetics, carbon fiber composites, fibrous materials, lithium-ion battery, multifunctional materials, self-sustaining materials

1 | INTRODUCTION

To combat climate change and environmental degradation in various sectors, ambitious targets have been set out to restrict CO_2 emissions. Electric vehicles (EV) are considered as one of the key solutions in reducing emissions from the transport sector. Main challenges for EV are cost and range. One solution to increase driving range is decreasing the vehicle mass by incorporating many functions in the same material.[1,2] In the literature, there are two main courses of action to achieve combined mechanical and electrical performance in structures. One approach is to add functionalities into a component, such as embedding thin-film batteries within composite laminates.[3–5] The obtained multifunctional sandwich structure relies on optimized assembly of monofunctional components. The resulting devices can be referred to as multifunctional components.[6] The second approach is to make a multifunctional composite material in which each constituent has inherent multifunctionality, that is, a multifunctional material.[6] Two types of such structural battery composite materials have emerged over the last decade.[7–14] The first type is a laminated device, in which one lamina constitutes a structural negative electrode and

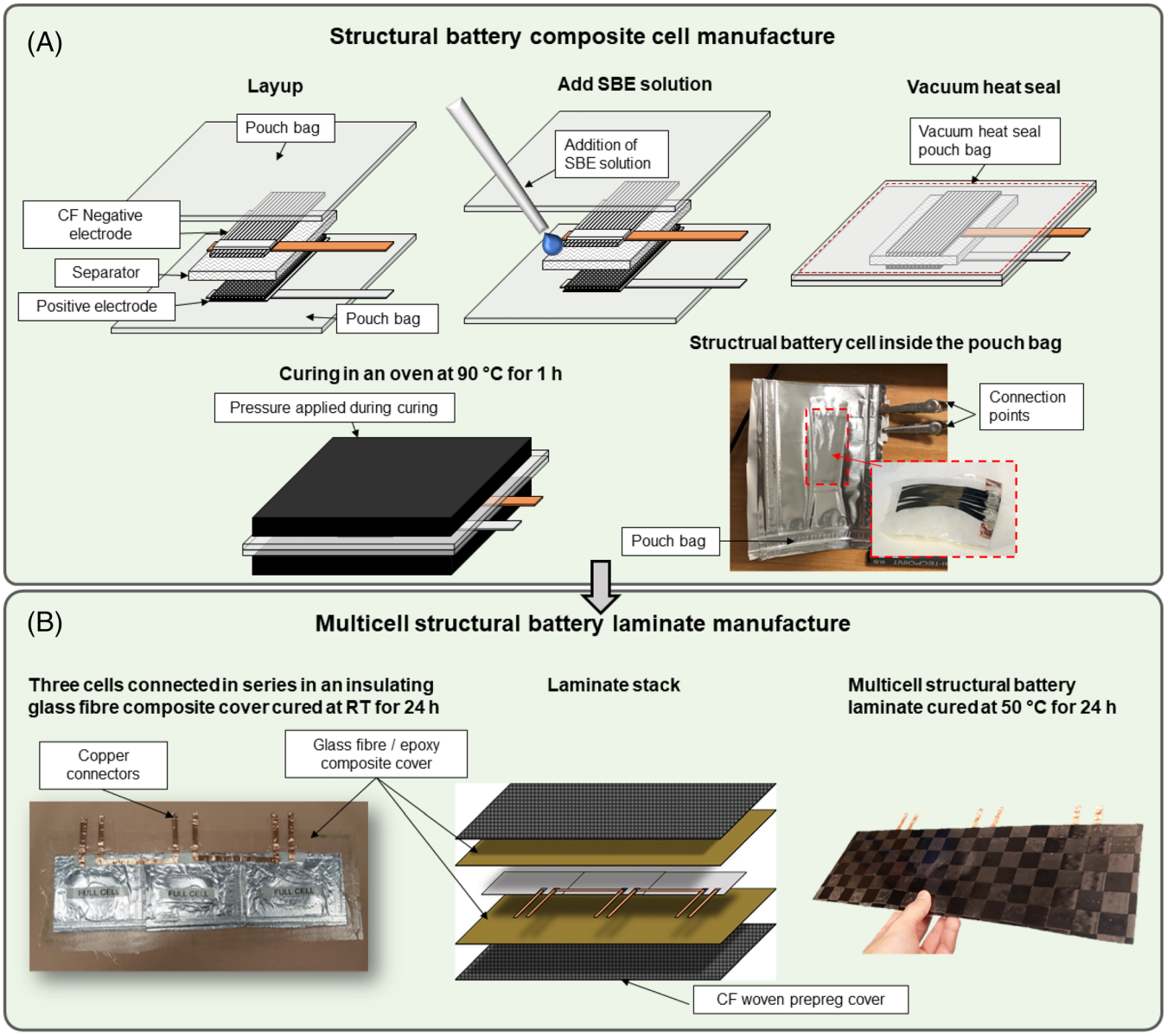

FIGURE 1 (A) Structural battery composite cells manufacture; and (B) Their connection, insulation, and installation in the multicell structural battery laminate

a structural positive electrode, separated by an electrically insulating separator ply.[7–10] The entire laminate is then impregnated by a structural battery electrolyte. One such structural battery composite material concept studied here employs carbon fibers for mechanical performance and as electrode, and uses a lithium (Li) ion conductive two-phase polymer electrolyte matrix for mechanical load transfer between fibers and for ion transport and electrical insulation between electrodes. The second type of structural battery composites is a micro-battery material utilizing a unidirectional array of individually polymer electrolyte coated carbon fibers in a cathode doped polymer matrix.[11–13] Dong and co-workers recently presented structural micro-battery devices manufactured by a 3D-printing technique.[12,13]

System level benefits from using structural battery composites in EV have been demonstrated by a recently developed performance analysis framework.[1] Life-cycle assessment undertaken to evaluate cradle-to-grave environmental impacts of structural battery composites found that climate impact, ozone formation and abiotic depletion in substantive quantities can be avoided.[15]

Recently, Asp et al. demonstrated a laminated structural battery composite cell, employing a structural battery electrolyte (SBE).[7] Its multifunctional properties surpassed all previous structural battery materials reported in the literature.[8–13] The structural battery composite material had an energy density of 24 Wh kg^{-1} (relative the total mass of the cell) and an elastic modulus of 25 GPa. To date, other

attempts to make laminated structural batteries have resulted in significantly lower elastic modulus.[8–10] Pappas et al. showed an increased longitudinal modulus for the 3D-printed batteries, but with low cell capacity.[13]

In spite of these recent achievements, numerous research questions and challenges remain to be addressed to further increase the material's performance and technology readiness level. One of the most important features of structural batteries is the retention of electrochemical performance after mechanical loading, and vice versa. To utilize structural battery composites in structural load paths, maintained electrochemical functionality after repeated mechanical load must be guaranteed. The stiff SBE restricts expansions of the active materials, that is, the carbon fibers and lithium iron phosphate (LFP) particles, that occur during a charge cycle.[7,14,16,17] It may therefore be damaged during electrochemical cycling, jeopardizing the electro-chemo-mechanical performance of the material.[18] Data to demonstrate electrochemical performance retention after mechanical loading of structural battery composites with a SBE matrix have not yet been presented. Here, electro-chemo-mechanical performance retention of the structural battery composite is demonstrated. For this purpose, a structural battery composite cell is designed and characterized, where mechanical tensile load cycles are alternated with galvanostatic charge/discharge (GCD) cycling.

When the electrical load requirement from a battery cell is greater than its output voltage or capacity, a combination of cells is required to serve the desired load. To date, no studies addressing multifunctional performance of structural battery composite devices made from multiple cells have been published. Multicell device performance is strongly affected by structural battery composite cell variability, connectivity, and power management solutions. The purpose of this work is to demonstrate the design and operation of a multicell structural battery composite laminate, with three cells connected in series. The current study extends from single battery cell scale, via connected multiple cells to encapsulated laminate scale as schematically illustrated in Figure 1. The total voltage of the system is the sum of the individual cell voltage, so that applications having higher voltage requirement can be operated. For batteries in serial connection, herein referred to as multicell structural battery laminate or structural battery pack, small differences in capacity among cells appear due to production tolerances. These differences tend to increase with each charge/discharge cycle. The battery self-discharge is another phenomenon considered in terms of contribution to an imbalance. When weaker cells are charged along stronger ones, the weaker cells become overstressed, which further increases the imbalance. This continuing imbalance causes an anomaly in capacity, until the weakest cell eventually fails. The need and approach for balancing cells to avoid damage formation and reduction in life is demonstrated. The structural battery composite cells and the multicell structural battery laminate are fabricated as shown in Figure 1. The composite laminae encapsulation of the structural battery composite cells is considered to calculate the in-plane engineering moduli for the structural battery laminate.

2 | RESULTS AND DISCUSSION

2.1 | Multifunctional performance of the structural battery composite cell

The structural battery composite cell tensile test specimen was designed to study the materials reversible battery performance following mechanical loading, and vice versa. Tensile tests were performed outside the pouch bag inside the glovebox. The specimen and test set up are shown in Figure 2. The capacity retention was studied via long-term cycling at 0.16 C. The long-term cycling performance was tested over 125 galvanostatic charge/discharge (GCD) cycles shown in Figure 2D. Prior to this, the cell had a cycling history corresponding to that reported by Asp et al., including preconditioning, cycling at different C-rates, and additional cycles, in total exceeding 100 cycles.[7] Hence, the cell shows high capacity retention after 200 GCD cycles.

Initial GCD measurements were recorded, prior to any mechanical loading, and then the battery composite specimen was mechanically loaded in tension to 0.18% strain, at which point the tensile testing was stopped, the specimen was unloaded and removed from the tester. The structural battery was placed back into a pouch bag with additional liquid electrolyte, to compensate for evaporation, and GCD cycling was performed. Subsequently, the composite was loaded to 0.36% and 0.51%, with alternating GCD cycling. In Figure 2E the effect of mechanical tensile loading on galvanostatic cycling is shown. The battery's potential is plotted versus specific capacity. The results show that the capacity of the battery composite is unaffected by tensile loading to 0.18% strain (blue solid line), but a small increase in cell resistance as an internal resistance (IR) drop can be observed. The discharge curve following a tensile load to 0.36% demonstrates further increase in IR-loss, while the capacity is only slightly reduced (dashed red line). Figure 2F shows the stress–strain curves of the discharged battery composite under tensile load with GCD cycles between each tensile test, respectively, with markers to indicate the terminations. The tensile test results show excellent repeatability for the tests with the slope of the curves coinciding. The

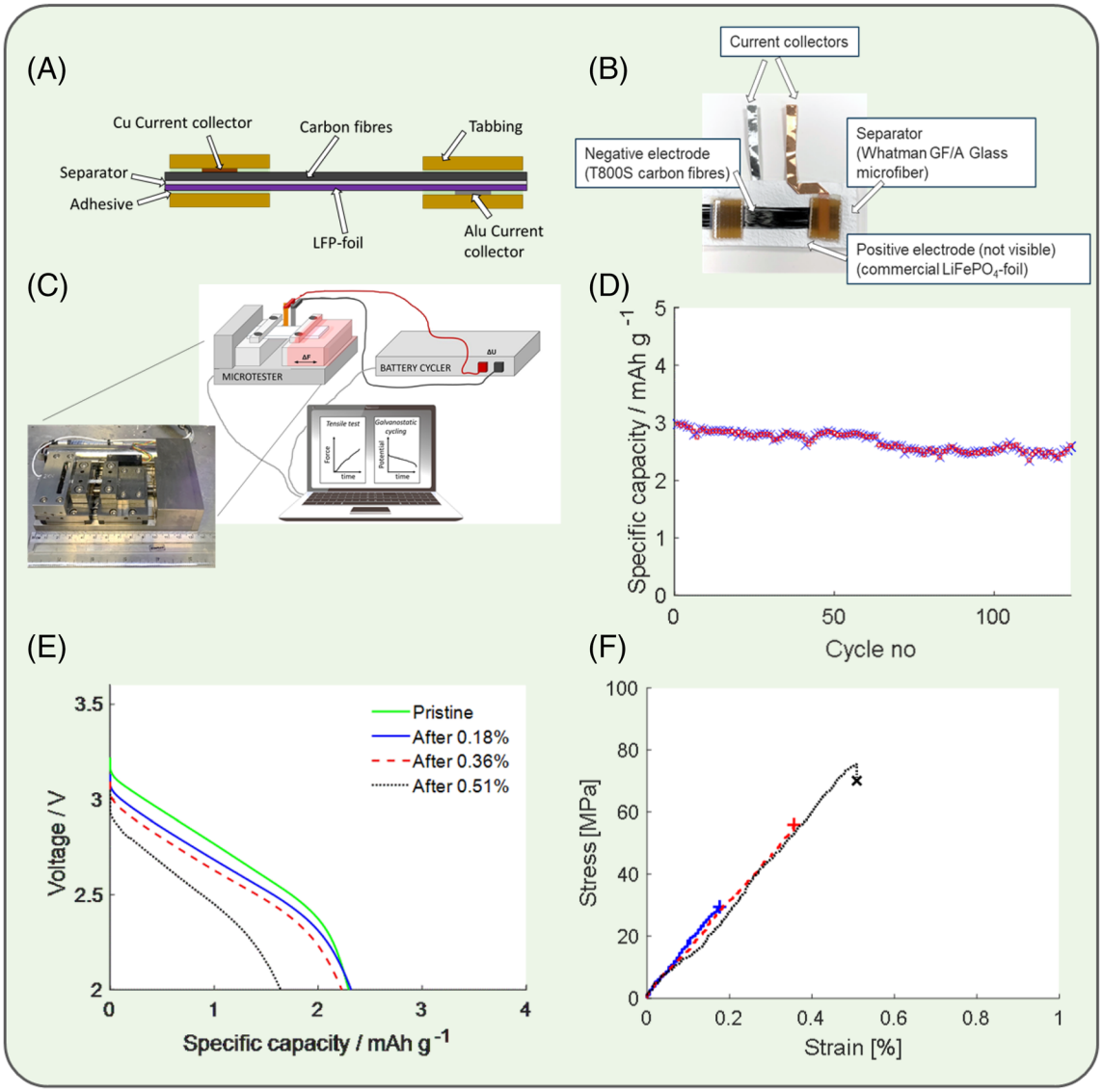

FIGURE 2 Multifunctional performance of the structural battery composite cell specimen. (A) Schematic illustration of the cell design; (B) Photograph of the manufactured sample; (C) The test specimen mounted in the Deben miniature test rig and schematic of the mechanical and electro-chemical test set up inside the glovebox; (D) Long term cycling at 0.16 C (capacity normalized to the total weight of the battery cell); (E) Galvanostatic discharge curves for the pristine cell and after subsequent mechanical load cycles: (F) Mechanical stress–strain curves for the discharged structural battery composite, tested at increased strain levels following intermittent galvanostatic charge/discharge cycles

tensile modulus of the battery composite in the fiber direction is 16.8 GPa, calculated from the strain range 0.1%–0.3% for the tests terminated at 0.36% and 0.51%, and 0.1%–0.15% for the test terminated at 0.18%. The measured tensile modulus is slightly lower than that reported by Asp et al. for the same cell type.[7] This is explained by changes in the test method introduced to allow for sequential mechanical and electrochemical tests in the current study.

From these results it is evident that the structural battery composite cells maintain their multifunctional performance capability also after being exposed to realistic mechanical load levels (a typical allowable strain level for carbon fiber composites is 0.4%).

2.2 | Multifunctional performance of the multicell structural battery laminate

The multicell structural battery laminate was assembled with three cells connected in series as illustrated in Figure 1B. A video demonstrating the combined mechanical and electrochemical function of the multicell structural battery laminate is presented in the Data S1.

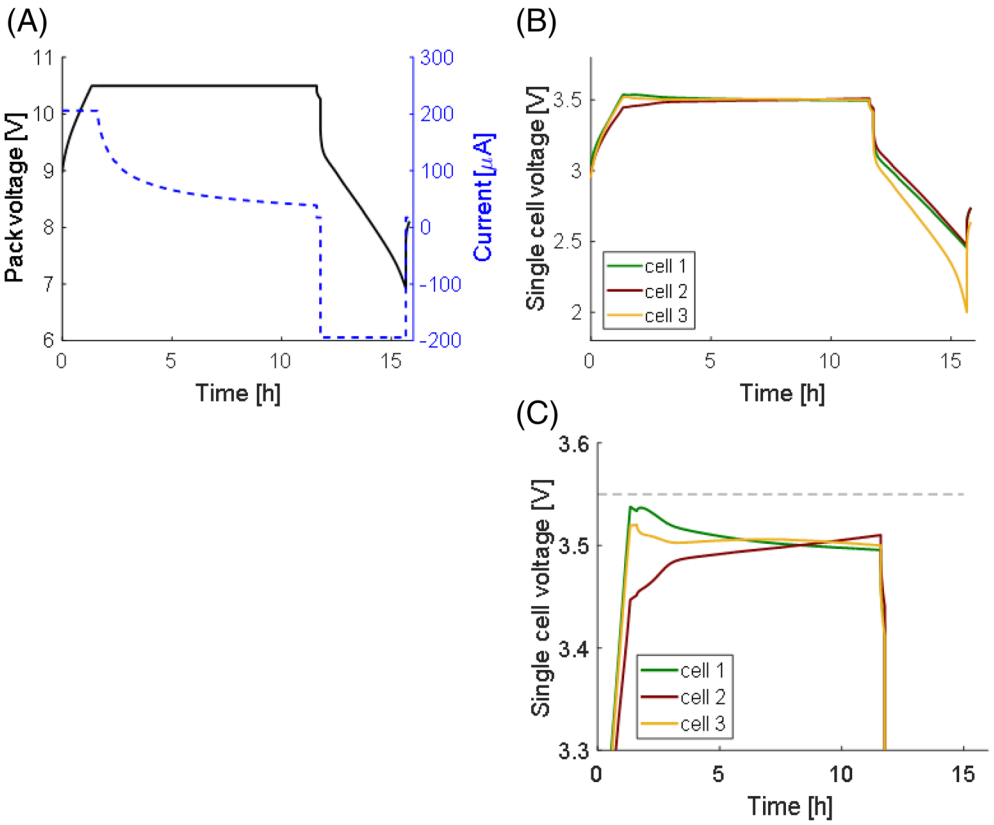

FIGURE 3 CCCV charge and galvanostatic discharge for: (A) The structural battery pack; (B) Each structural battery composite cell individually; and (C) A close up of the cell voltage for the individual cells

2.2.1 | Electrochemical performance

In Figure 3 the constant current constant voltage (CCCV) charge/discharge of the structural battery pack without a battery management system (BMS) is shown. Figure 3A shows the voltage and current for the whole pack, and Figure 3B depicts the voltage curves of the individual cells. Since the cells are connected in series, the current through each cell is the same as through the battery pack.

The maximum voltage of a single cell was set to 3.55 V. Thus, in theory the maximum voltage of the pack can reach 10.65 V. However, for safety, since there was no balancing circuit in this first setup, the maximum voltage limit of the whole battery pack was set to 10.5 V. During the constant voltage charge phase, the voltage of Cell 1 and Cell 2 decreases slightly due to the leakage current at high state of charge (SOC). The voltage gap caused by the self-discharge in these cells allowed Cell 3, which is the weak cell, to continue to charge. In this way, the cells became balanced without a BMS circuit. Although the balancing function of the leakage current was adequate, the set voltage limit did not allow for the battery pack to be fully charged. In fact, the charging procedure was stopped as soon as one of the cells reached the cell cut-over voltage. As shown in Figure 3B and Figure 3C, employing a safe voltage limit of 10.5 V, none of the cells reached 3.55 V. As further illustrated in Figure 3B, during discharge, the difference in performance of the structural battery composite cells is significant, where cell 3 first reached the cut-off voltage, 2 V, and thus limited the usable capacity of the complete structural battery pack.

To mitigate problems caused by the variation in electrical performance of the three structural battery composite cells a BMS utilizing passive balancing of the cells was used. The implemented BMS allowed the structural battery pack to be fully charged. Schematics of the BMS set up and connection of cells are presented in Figure 4.

The impedance of the structural battery pack at different SOC, measured with an electrochemical impedance spectroscopy (EIS) technique, is shown in Figure 5A. At a high frequency, the battery system has a pure resistive behavior (the imaginary part is zero). With the frequency decreasing, the battery shows a capacitive character due to the double layer capacitance. The double layer capacitor and the charge transfer resistance form a parallelly connected RC link (combination of a resistor and capacitor in the electrical equivalent circuit representation) and thus result in a semi ellipse in the impedance plot, as shown in Figure 5A. The reason for the semi ellipse shape instead of a semi-circle shape is that the double layer capacitance is nonlinear. Impedance results for the individual cell are plotted in Figure 5B. A significant difference in cell resistivity is evident. Figure 5C,D show that the battery impedance increases as the frequency

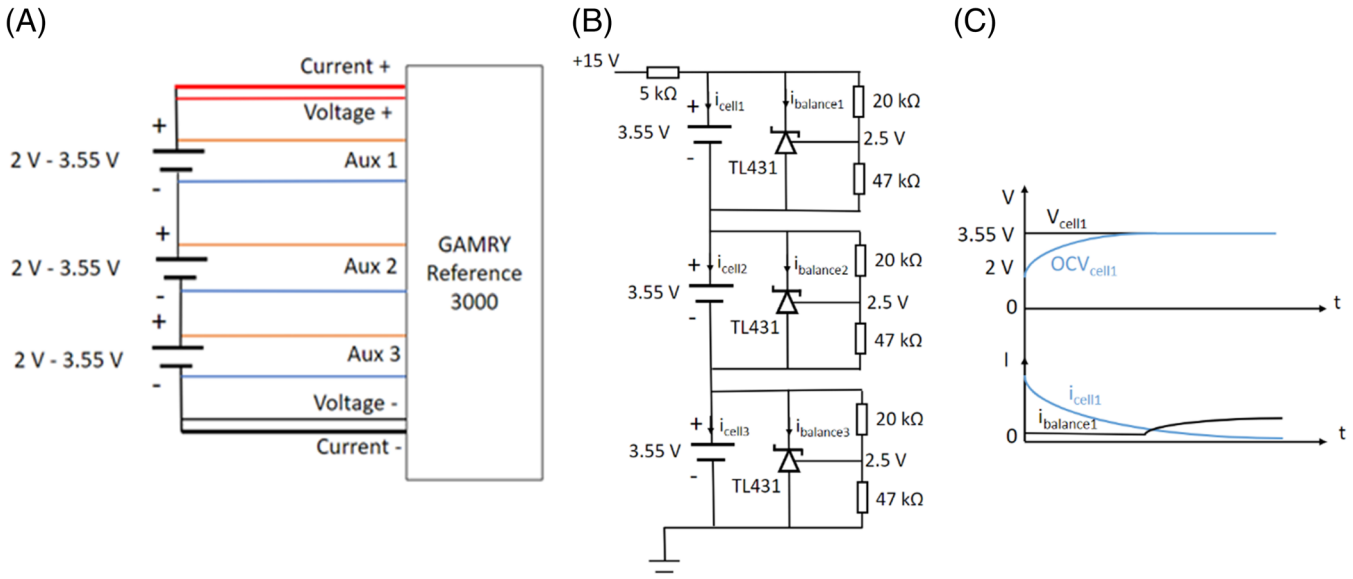

FIGURE 4 Schematics of the battery cells connected in series. (A) A four-wire measurement was used for the battery pack during CCCV charging and auxiliary channels were used for each cell individually; (B) Setup with BMS using passive balancing with a voltage reference regulator TL431 connected in parallel with dividing resistors R1 (=20 kΩ) and R2 (=47 kΩ); (C) Working principle of the passive balancing in the BMS

decreases. The three cells have a similar impedance magnitude at high frequency, whereas the impedance deviates between the cells at low frequency. The capacitive behavior of the structural battery pack and the individual structural battery composite cells are depicted in Bode plots in Figure 5E,F for the considered frequency range.

Furthermore, the impedance at high frequency is related to the ionic resistance of the electrolyte and the electronic resistance of the electrodes and current collectors, which is independent from the battery SOC. This is reflected in the measurement where the solid lines and dashed lines are overlapped at the high frequency points. On the other hand, the length of the semi ellipse that reflects the magnitude of the charge transfer resistance is affected by the SOC. Typically, the charge transfer resistance at the lower SOC level is higher than the resistance at the higher SOC level.[19] The results for the structural battery pack, as well as the individual structural battery cells, show the same trend as reported in the literature for conventional cells. The measured surface impedance for the structural battery pack, considering a surface area of each cell of 4.5 cm,^{2} is in the range of 2700 to 4500 Ω cm.^{2} This is high compared to high-performance commercial lithium-ion batteries, which have a surface impedance in the range of 16–32 Ω cm^2 at high and low SOC, respectively.[20] The higher surface impedance of the structural battery pack stems from the lower ion conductivity of the SBE compared to the liquid electrolytes used in commercial batteries. Also, the lower electron conductivity of carbon fibers compared to copper adds to the electrical losses in the structural battery composite cells.

2.2.2 | Mechanical performance

The multicell structural battery laminate, and its layup, is depicted in Figure 1B. The laminate consists of a 0.10 mm thick carbon fiber plain weave sub-laminate [0/90], two glass fiber plain weave laminae (each 0.070 mm thick), placed on each side of the structural battery cells in their pouch bags (bag thickness of 0.096 mm). The structural battery cell placed in the middle of the laminate has a thickness of 0.40 mm. The total laminate thickness, H, was 1.07 mm. The multicell structural battery laminate was approximately 370 mm long and 120 mm wide. The elastic properties of the individual material layers are presented in Table 1.

Given the large in-plane dimensions of the multicell structural battery laminate no tensile tests could be performed to measure its in-plane mechanical properties. Instead, the effective elastic modulus, in the length and width directions, as well as in-plane shear modulus are estimated with classical laminate theory (CLT), using material properties listed in Table 1.

We use general expressions based on CLT to estimate the in-plane engineering elastic moduli of the

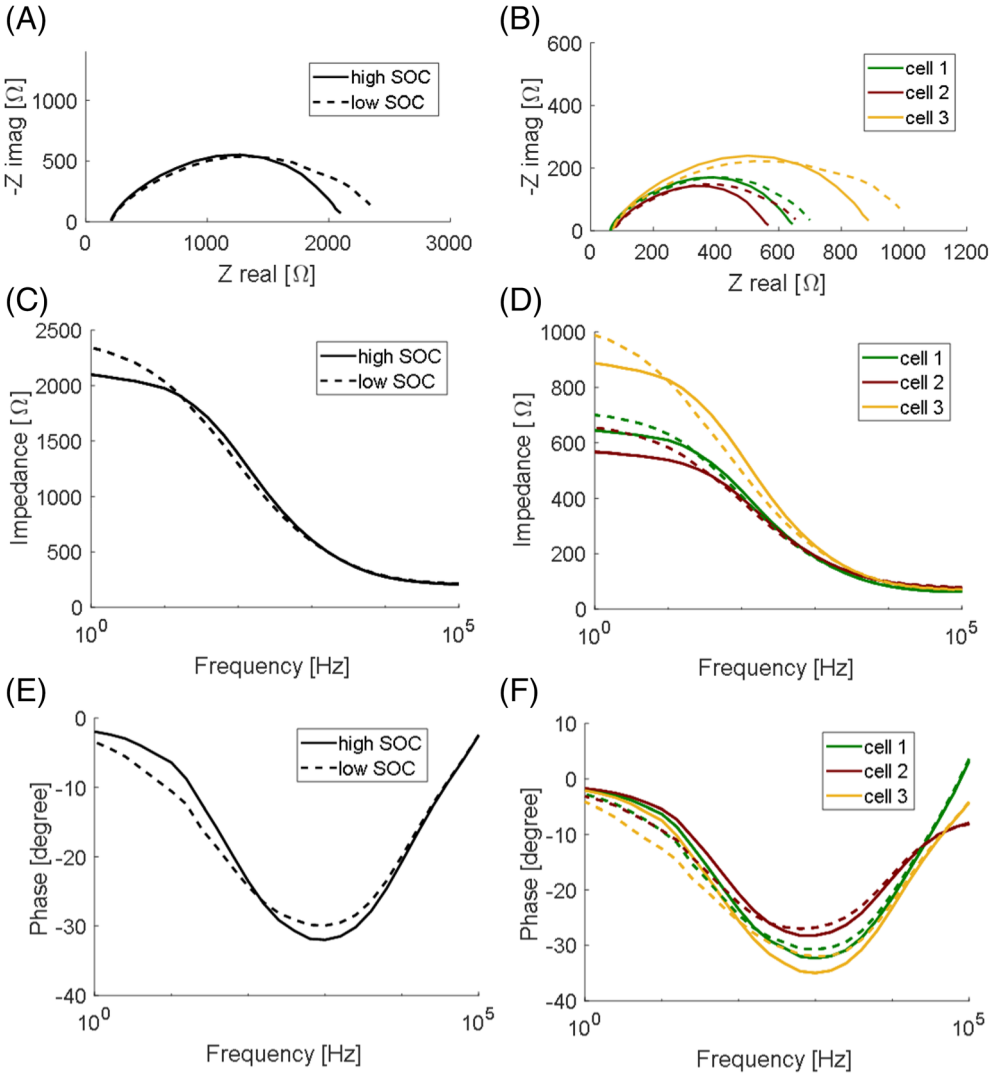

FIGURE 5 EIS measurements at different state of charge (SOC) for: (A) The structural battery pack; and (B) Each cell individually. Bode plots of the EIS measurements; (C) Impedance vs. Frequency for the structural battery pack at high and low SOC; (D) Impedance magnitude vs. Frequency for the individual structural battery composite cells; (E) Phase vs. Frequency for the structural battery back at high and low SOC; and (F) Phase vs. Frequency for the individual structural battery composite cells

TABLE 1 Material layer (lamina) in-plane elastic properties. The elastic properties for the carbon fiber and glass fiber woven lamina are provided by the suppliers. Subscripts L and T are parallel to the x- and y-directions, respectively. The properties of the pouch bag were estimated based on its material composition and the properties of the structural battery cell were reported by Asp et al.[7]

Material layer	E_L [GPa]	E_T [GPa]	G_{LT} [GPa]	ν_{LT} [−]
Carbon fiber lamina	148	9.65	4.55	0.30
Glass fiber woven lamina	19.0	19.0	4.20	0.13
Pouch bag	1.50	1.50	0.57	0.32
Structural battery composite cell	18.3	2.96	2.30	0.30

multifunctional structural battery laminate, presented by Farooq and Myler.[21] The effective moduli are calculated from the components of the A-matrix. The complete computations of the A-matrix (commonly referred to as the extensional stiffness matrix) and effective moduli are reported in the Data S1. The engineering modulus along the multicell structural battery laminate, $\overline{E}_x$, is calculated as

$$\overline{E}_x = \frac{1}{a_{11}H}, \tag{1}$$

where

$$a_{11} = \frac{A_{22}}{A_{11}A_{22} - A_{12}^2}. \tag{2}$$

The resulting engineering modulus along the multicell structural battery laminate, $\overline{E}_x$, is 26.9 GPa.

The engineering modulus across the width of the plate, that is, in the y-direction (c.f. Figure S1), is

$$\overline{E}_y = \frac{1}{a_{22}H}, \tag{3}$$

where

$$a_{22} = \frac{A_{11}}{A_{11}A_{22} - A_{12}^2}. \tag{4}$$

The resulting $\overline{E}_y$ is 21.1 GPa.

Finally, the engineering shear modulus of the multicell structural battery laminate, $\overline{G}_{xy}$, is calculated as

$$\overline{G}_{xy} = \frac{1}{a_{66}H}, \tag{5}$$

where

$$a_{66} = \frac{1}{A_{66}}. \tag{6}$$

The resulting engineering shear modulus of the multicell structural battery laminate, $\overline{G}_{xy}$, is 2.91 GPa.

The computed engineering moduli are reasonable for a hybrid laminate, and the laminate is considered suitable as a construction material. However, it should be recognized that the inclusion of pouch bags, with their PET/PE outer and inner surfaces, is undesired and will impair the mechanical performance of the laminate. In particular, the interfacial shear strength and load transfer is expected to be low at the structural battery cell/pouch bag interface. Consequently, the interlaminar strength and compression strength of the laminate are expected to be low.[22] Therefore, the pouch bags must be replaced by thin structural barrier layer(s) in future devices. Such barrier layers are still to be developed. For this reason, no strength estimates are made for the multicell structural battery laminate in the current study.

3 | CONCLUSION

Electrochemical performance retention of structural battery composite cells is demonstrated for repeated tensile loading. The capacity of the structural battery composite cell is found unaffected by the applied tensile loading at realistic mechanical load levels. A multicell structural battery laminate is realized embedding three structural battery composite cells connected in series between carbon fiber/glass fiber composite face sheets. To mitigate problems caused by a variation in charge transfer resistance between cells a battery management system with a balancing circuit is proposed. Electrochemical performance of the multicell structural battery is demonstrated. However, a significantly higher surface impedance is observed for the structural battery pack compared to that for commercial high-performance lithium-ion battery packs. This calls for improved structural battery electrolyte solutions, reduced separator thickness, and improved electron connector solutions. Finally, computed in-plane engineering moduli for the multicell structural battery laminate are on par with conventional monofunctional glass fiber composite multiaxial laminates. To further improve the mechanical properties thin structural barrier layers, to replace the pouch bags, must be developed.

4 | EXPERIMENTAL SECTION

4.1 | Materials

As negative electrode, an ultra-thin unidirectional PAN-based carbon fiber spread tow was used. Oxeon AB, Sweden, supplied the T800SC-12 k-50C carbon fiber spread to approximately 15 mm in width with a linear weight of 0.52 g m^{-1}. For the positive electrode, Lithium-Iron-Phosphate (LFP) single-sided coated electrode foil (with a specific capacity of 150 mAh g^{-1}) was purchased from Custom Cells Itzehoe GmbH, Germany. A glass microfibre separator (Whatman GF/A, 260 μm thickness) was used. The bi-continuous structural battery electrolyte (SBE) includes the following constituents: for the polymer material part Bisphenol A ethoxylate dimethacrylate (M_n: 540 g mol^{-1}) was supplied by Sartomer Europe; for the liquid electrolyte part propylene carbonate (PC) (PC ≥99%, acid <10 ppm, H_2O < 10 ppm) and ethylene carbonate (EC) (99% anhydrous) supplied by Sigma-Aldrich were used. Furthermore, for the SBE lithium trifluoromethanesulfonate (LiTf) (99.99%), Lithium bis(oxalato)borate (LiBoB) and 2,2′-azobis(2-methylpropionitrile) (AIBN) purchased from Sigma Aldrich were used. All materials were used as received. Copper foil and *aluminum* foil were used as current collectors of the negative and positive electrode, respectively. While PELCO® conductive silver paint was used to connect the copper foil to the fibers.

4.2 | Structural battery composite cell preparation

The structural battery composite cells were manufactured as schematically illustrated in Figure 1. Two types of cells were made. Firstly, structural battery cells were prepared for use in the multicell structural battery laminate. These structural battery composite cells were identical to those previously reported by Asp et al.[7] In these cells the electrodes were cut in dimensions of 30 mm × 10 mm. This corresponds to approximately 19 mg of carbon fibers and

38 mg of LFP particles in the complete battery cell. Secondly, structural battery composite cells were made for sequential electrochemical and mechanical tensile tests. Slender tabbed test specimen dimensions were adapted to fit the test equipment, with the dimensions 23 mm × 5 mm × 0.3 mm (length × width × thickness).

All cells were prepared the same way. The battery cell constituents were placed inside a pouch laminate bag (PET/Al/PE, 12 μm/ 9 μm/75 μm thick) to avoid any exposure to air and moisture. Copper foil and *aluminum* foil were used as current collectors of the negative and positive electrode, respectively. While PELCO® Conductive Silver Paint was used to connect the copper foil to the fibers, the aluminum foil was connected to the LFP foil solely by applying pressure during manufacturing. The separator was, cut slightly larger than the two electrodes to prevent short circuit. The structural battery cell constituents were impregnated with the SBE solution using a pipette before vacuum heat-sealing the pouch-bag. The SBE solution was made by mixing 50:50 wt % of (i) a liquid electrolyte solution made from the mixture of LiBoB and LiTf at concentrations of 0.4 and 0.6 M, respectively, in EC:PC 1:1 w/w (50:50 wt %) and (ii) monomer bisphenol A ethoxylate dimethacrylate and the thermal initiator, AIBN (1 wt % of the monomer weight). The SBE solution was prepared in accordance with the procedure described by Asp et al.[7] To achieve a homogeneous solution, the SBE mixture was stirred using a vortex before it was added to the battery cell. Once the pouch-bag was vacuum heat sealed it was transferred to a preheated oven outside the glovebox and thermally cured at 90°C for 60 min. During thermal curing pressure was applied on the cells using clamps.

Three structural battery composite cells were manufactured and introduced in the multicell structural battery laminate. In addition, two structural battery composite cells aimed for electrochemical retention tests, following intermittent tensile tests, were manufactured. The retention test specimens were tabbed using glass fiber composite tabs, as illustrated in Figure 1. The tabs allow the specimens to be gripped in a tensile tester, *Deben UK* micro-tensile tester. DeltaPreg AX003 epoxy adhesive was used to adhere the materials between the tabs. On one end of the specimen, Cu current collector, carbon fiber tow, separator, and LFP-foil. On the other end, CF tow, separator and LFP-foil connected to an Alu current collector, Figure 2A. The resulting specimens were heat-cured at 90°C for 60 min and dried overnight at 50°C under vacuum before placed in an argon filled glovebox. SBE was added to the specimen and the electrochemical cell was vacuum sealed in a pouch bag and cured following the procedure as described in the previous paragraph.

4.3 | Multicell structural battery laminate preparation

The preparation of the multicell structural battery laminate was made in two steps, as illustrated in Figure 1. In a first step, the three electrochemically conditioned structural battery cells connected in series using copper strips were laminated between two layers of woven glass fiber fabric using wet layup with low temperature curing epoxy (NM Infusion 664, supplied by Nils Malmgren AB, Sweden) and cured under vacuum at room temperature for 24 h. The purpose of glass fiber composite laminate is to ensure electrical insulation of the cells and the connections, which is the reason why a follow-up check of leaking currents was carried out. In the next step, the glass fiber composite laminate with the encapsulated structural battery cells was laminated between two layers of low temperature curing carbon fiber LTC102 prepreg, supplied by Oxeon AB. The multicell structural battery laminate was cured under vacuum at 50°C for 24 h.

4.4 | Multifunctional performance tests of the structural battery composite cell

The specific capacity of the structural battery cells was measured by means of repeated galvanostatic charge and discharge (GCD) cycles using a Neware CT-4008-5V10mA-164 battery cycler. The cells were cycled between 2.00 and 3.55 V. Between each charge and discharge cycle a resting time of 60 min was used to allow ion-concentration gradients to relax. The capacity retention of the structural battery composite cell was studied via long-term galvanostatic charge/discharge (GCD) cycling at a current density of 3.51 mA g^{-1} corresponding to 0.16 C. Prior to the long-term cycling performance test, the cell has a cycling history corresponding to what was reported by Asp et al., including preconditioning, cycling at different C-rates and additional cycles, in total exceeding 100 cycles.[7] Tensile tests were carried out on the tabbed structural battery composite specimens at discharged state inside the glovebox. The structural battery was removed from the pouch bag and mounted in a micro tester for mechanical characterization. Here, a Deben 2 kN tensile stage was used. The used set up does not provide the possibility of using conventional techniques for measuring strain. For that reason, the applied strain is obtained directly form the tester crosshead displacement of the micro tester. Tensile tests were performed under displacement control at a rate of 0.1 mm min^{-1}.

4.5 | Electrochemical tests of the multicell structural battery laminate

The electrochemical performance of the multicell structural battery laminate was characterized using a GAMRY Reference 3000. A four-wire measurement setup was implemented to exclude the impedance from the current carrier cables. To assess the performance of each cell individually, auxiliary channels were used, as illustrated in Figure 4A. The voltage range of a single cell is 2.0–3.55 V and the upper voltage limit of the multicell pack is 10.5 V. The multicell structural battery laminate pack was charged with the constant current constant voltage (CCCV) procedure and discharged with a constant current. Besides the cycling test, the electric impedance was investigated to evaluate the power capability of the battery system. The structural battery system is a nonlinear system, meaning the battery impedance is changing with the frequency. Therefore, the electrochemical impedance spectroscopy (EIS) technique was used in this work where the impedance response at each frequency can be observed separately. The EIS measurement was applied at different states of charge (SOC) to analyze the impedance of the multicell structural battery laminate pack, as well as the individual cells.

4.6 | Battery management system

The cells were manufactured manually in a lab environment, and thus there was a significant variation between samples, both in terms of the capacity and the internal impedance, as shown in the cycling graphs in Figure 3B. Since the cells are connected in series, the current passing through the cells is the same, while the impedance and capacity difference will cause different terminal voltages for each cell. During charging, the cell with the lowest capacity/largest impedance will reach the cut-off voltage first. Without a battery management system (BMS), the charge event is limited, and the other cells cannot be fully charged. Therefore, a setup with a BMS was found to be necessary in this work to balance the cells during charging.

In this work, passive balancing is utilized with a voltage reference regulator TL431 connected in parallel with dividing resistors, Figure 4B. The reference voltage of TL431 is 2.5 V and the output voltage is set to be the maximum voltage of the cell 3.55 V. The dividing resistors R1 and R2 were chosen to be 20 and 47 kΩ according to

$$V_{out} = \frac{(R_1 + R_2)}{R_2} \cdot V_{ref} \tag{7}$$

Theoretically the resistors can have any value if Equation (7) is fulfilled. In practice, the resistors are preferred to have a higher value to limit the current and reduce the power loss.

When the battery pack is charged with this circuit, there is no need to use a dedicated potentiostat. Instead, a regular 15 V power supply is connected directly to the circuit. The voltage reference TL431 will regulate the voltage over the structural battery composite cells to be 3.55 V constantly, therefore any power supply with an output above 10.65 V can be used for charging. There is a 5 kΩ resistor at the power supply set to take the excess voltage.

During charging, each cell is applied with a constant voltage once the voltage over an individual cell reaches its maximum, and the charging current is naturally limited by the internal impedance of the cell itself. When the voltage of a single cell reaches 3.55 V, the regulator will bypass the current to prevent the output voltage from exceeding the limit. This will not affect the remaining cells but eventually allow all the cells in the battery pack to become fully charged.

ACKNOWLEDGMENTS

This project has been funded by the European Union, Clean Sky Joint Undertaking 2, Horizon 2020 under Grant Agreement Number 738085, USAF contract FA8655-21-1-7038, the National Swedish Energy Administration project 42789-1, and the Swedish National Space Agency, contract 2020-00256. Financial support from Chalmers' Area of Advance Energy and LIGHTer Academy via VINNOVA is also gratefully acknowledged.

CONFLICT OF INTEREST

The authors declare no conflict of interest.

ORCID

Leif E. Asp https://orcid.org/0000-0003-0630-2037

REFERENCES

1. Carlstedt D, Asp LE. Performance analysis framework for structural battery composites in electric vehicles. *Compos Part B Eng*. 2020;186:107822.
2. Johannisson W, Zenkert D, Lindbergh G. Model of a structural battery and its potential for system level mass savings. *Multifunct Mater*. 2019;2(3):035002.
3. Thomas J, Qidwai S. Mechanical design and performance of composite multifunctional materials. *Acta Mater*. 2004;52(8):2155-2164.
4. Thomas J, Qidwai S, Pouge W III, Pham G. The design and application of multifunctional structure-battery materials systems. *JOM*. 2005;57(3):18-24.
5. Ladpli P, Nardari R, Kopsaftopoulos F, Chang FK. Multifunctional energy storage composite structures with embedded lithiumion batteries. *J Power Sources*. 2019;414:517-529.

6. Asp LE, Greenhalgh ES. Structural power composites. *Compos Sci Technol*. 2014;101:41-61.
7. Asp LE, Bouton K, Carlstedt D, et al. A structural battery and its multifunctional performance. *Adv Energy Sustain Res*. 2021; 2(3):2000093.
8. Meng C, Muralidharan N, Teblum E, Moyer KE, Nessim GD, Pint CL. Multifunctional structural ultrabattery composite. *Nano Lett*. 2018;18(12):7761-7768.
9. Moyer K, Meng C, Marshall B, et al. Carbon fiber reinforced structural lithium-ion battery composite: multifunctional power integration for CubeSats. *Energy Storage Mater*. 2020;24:676-681.
10. Liu P, Sherman E, Jacobsen A. Design and fabrication of multifunctional structural batteries. *J Power Sources*. 2009; 189(1):646-650.
11. Asp LE, Leijonmarck S, Carlson T, Lindbergh G. Realisation of structural battery composite materials, ICCM 20, 20th International Conference on Composites, Copenhagen, Denmark. 2015.
12. Thakur A, Dong X. Printing with 3D continuous carbon fiber multifunctional composites via UV-assisted coextrusion deposition. *Manuf Lett*. 2020;24:1-5.
13. Pappas JM, Thakur AR, Dong X. Effects of cathode doping on 3D printed continuous carbon fiber structural battery composites by UV-assisted coextrusion deposition. *J Compos Mater*. 2021;55(26):3893-3908.
14. Schneider LM, Ihrner N, Zenkert D, Johansson M. Bicontinuous electrolytes via thermally initiated polymerization for structural lithium ion batteries. *ACS Appl Energy Mater*. 2019;2(6):4362-4369.
15. Zackrisson M, Jönsson C, Johannisson W, et al. Prospective life cycle assessment of a structural battery. *Sustain*. 2019;11:1-14.
16. Ihrner N, Johannisson W, Sieland F, Zenkert D, Johansson M. Structural lithium ion battery electrolytes: via reaction induced phase-separation. *J Mater Chem A*. 2017;5(48):25652-25659.
17. Duan S, Iyer AHS, Carlstedt D, et al. Effect of lithiation on the elastic moduli of carbon fibres. *Carbon*. 2021;185:234-241.
18. Xu J, Varna J. Matrix and interface cracking in cross-ply composite structural battery under combined electrochemical and mechanical loading. *Compos Sci Technol*. 2020;186:107891.
19. Geng Z, Thiringer T, Olofsson Y, Groot J, West M. On-board impedance diagnostics method of li-ion traction batteries using pseudo-random binary sequences, 2018 20th European Conference on Power Electronics and Applications, EPE 2018 ECCE Europe. 2018; 1–10.
20. Wikner E. Ageing in Commercial Li-Ion Batteries: Lifetime Testing and Modelling for Electrified Vehicle Applications, Doctoral thesis, Chalmers University of Technology, Gothenburg, Sweden. 2019.
21. Farooq U, Myler P. Efficient determination of mechanical properties of carbon fibre-reinforced laminated composite panels. *ARPN J Eng Appl Sci*. 2017;12(5):1375-1392.
22. Nilsson K-F, Asp LE, Alpman JE, Nystedt L. Delamination buckling and growth for delaminations at different depths in a slender composite panel. *Int J Solids Struct*. 2001;38(17):3039-3071.

SUPPORTING INFORMATION

Additional supporting information may be found in the online version of the article at the publisher's website.

How to cite this article: Xu J, Geng Z, Johansen M, et al. A multicell structural battery composite laminate. *EcoMat*. 2022;e12180. doi:10.1002/eom2.12180